DESIGN OF A SOFT X-RAY FEL IN THE SLAC A-LINE

H. Geng*,Y. Ding, P. Emma, J. Galayda, Z. Huang and Y. Nosochkov
SLAC, Menlo Park, CA 94025, USA

Abstract

LCLS capabilities can be significantly extended with a second undulator aiming at the soft X-ray spectrum (1- 5 nm). To allow for simultaneous hard and soft X-ray operations, 13.6 GeV beams at the end of the LCLS accelerator can be intermittently switched into the SLAC A-line (the beam transport line to End Station A) where a second undulator may be located. Recently, a new optics has been designed to transport the LCLS beam through the A-Line while preserving the beam brightness. In this paper, we discuss the A-Line soft X-ray FEL design — parameter selection and performance expectations with an energy-chirped LCLS beam as required by the A-Line optics. Start-to-end simulations using realistic LCLS beams show that it is possible to generate 70 GW FEL power with a pulse duration as short as 2 fs at 20 pC charge.

INTRODUCTION

The Linac Coherent Light Source (LCLS) has recently achieved lasing and saturation at 1.5 Å [1], and it will soon start supplying light to users. At any given time the new laser will be able to produce light in the spectral range 15–1.5 Å by adjusting the final beam energy in the range 4.3–13.6 GeV. Initially the LCLS will be a single undulator X-ray source that will provide either hard or soft X-rays of a specific wavelength to users at a time. As there is a great demand for both hard and soft X-rays, however, it is worth considering a future expansion of the LCLS to provide both types of X-rays at the same time, in a scenario where a 13.6 GeV beam can be shared between the current LCLS undulator—where it generates hard X-rays—and a new beamline and undulator—where it will generate soft X-rays. The existing SLAC A-Line [2] is a prime candidate location for such a soft X-ray beamline and undulator.

The A-Line was designed to deliver high energy electron beams (up to 50 GeV) to fixed target experiments in the End Station A experimental hall. The tunnel and all existing magnets in the A-Line can be used for the new soft X-ray FEL, and no new civil construction is necessary. A major difficulty with using the A-Line for an FEL is that it bends through a total angle of 24.5°, therefore transporting a high current, high brightness LCLS beam through it without degrading beam quality is a major challenge. Incoherent and Coherent Synchrotron Radiation (ISR and CSR) in the bending section will generate energy spread, which may couple to the transverse (bending) plane and increase the beam emittance, and thus degrade the free electron laser performance.

The possibility of installing an undulator in the A-Line in order to create a soft X-ray FEL aiming at the spectral range (1–5 nm) has been considered in a recent report [3]. In that report the transport of a 13.6 GeV LCLS beam through the A-Line was studied in detail, considering both single-particle and collective effects. A new lattice was designed for transporting the LCLS beam through the existing tunnel while preserving the beam quality. The new lattice requires an over-compressed beam after the second bunch compressor of the LCLS. The beam is then further compressed in the bends of the A-line. Simulations show that the ISR and CSR effects are well suppressed in the new lattice. Note that in this scheme the beam arrives at the undulator with a linear energy chirp.

In the present paper, we continue the work of designing a Soft X-ray FEL in the A-Line but focusing on the undulator region: we transport the beam through to the end of the undulator and study the FEL performance. At the end we also compare the effectiveness of using a permanent magnet, planar undulator *vs.* a superconducting helical type.

In Table 1 we present beam and photon parameters for the A-Line soft X-ray FEL assuming a planar, variable gap, permanent magnet undulator. For our simulations we consider bunch charges of $Q = 250$ pC—the nominal LCLS value—and $Q = 20$ pC—a low charge option that promises a single spike radiation pulse [4]; in both cases the beam energy is 13.6 GeV.

PARAMETER SELECTION

The A-Line soft X-ray FEL should meet the following requirements: First, the radiation spectrum should cover 1-5 nm at a fixed electron energy of $E_0 = 13.6$ GeV, to be compatible with the LCLS hard X-ray program. Second, the FEL saturation length should be no more than 80 meters due to the space limitation in the A-Line.

The radiation wavelength of an FEL is determined by the resonant condition: $\lambda_s = \frac{\lambda_u}{2\gamma^2}(1 + K^2/2)$, where λ_s is the radiation wavelength, λ_u is undulator period, γ is the electron beam energy relative to its rest mass, and $K = 0.934\lambda_u[cm] \cdot B_u[T]$ is the undulator parameter with B_u the peak magnetic field of the undulator. The period and range of magnetic field in the undulator are significantly constrained by the combination of beam energy of 13.6 GeV and the radiation wavelength of $\lambda_r = 5$ nm. A conventional planar (hybrid) permanent magnet undulator with a peak magnetic field of 1.7 T (near the practical limit for this technology) will have a period of $\lambda_u = 8$ cm.

* Email: genghp@slac.stanford.edu. Visiting SLAC from University of Science and Technology of China.

Table 1: Main Parameters for A-Line Soft X-ray FEL

Parameter	symbol	value	unit
Electron energy	E_0	13.6	GeV
Repetition rate	f	60	Hz
Norm. rms emittance	$\epsilon_{nx,y}$	~ 1	μm
Peak current	I_{pk}	3–5	kA
Bunch charge	Q	20–250	pC
Final bunch length	σ_{zf}	1–10	μm
Slice energy spread	$\sigma_{\delta s}$	0.01–0.04	%
Undulator period	λ_u	8	cm
Undulator parameter	K	5–13	
Mean undulator β func.	$\langle\beta\rangle$	10	m
FEL wavelength	λ_r	1–5	nm
Photon energy	$\hbar\omega$	0.25–0.12	keV
FEL power	P_{FEL}	~100	GW
FEL bandwidth(FWHM)	$\Delta\omega/\omega$	0.3–1	%
Pulse length (FWHM)	$\Delta\tau$	2–50	fs
Energy per pulse	E_{FEL}	0.1–2	mJ
# of photons/0.1%BW	N_γ	$1-10$	10^{12}
Peak brightness	B_{pk}	5–30	10^{31*}

*# of photons/mm^2/mrad^2/sec/0.1%

Shorter wavelength radiation can be produced by opening the gap of the undulator. However, the longitudinal space available for the undulator, 80 meters, limits the "harder" end of the undulator radiation spectrum to about 1 nm, as will be shown later.

We choose a FODO lattice for focusing in the undulator region because of its simplicity. The smaller the beam size, the larger the electron density and the FEL parameter ρ [5], and therefore the better the FEL performance. However, 3D effects, especially diffraction, will begin to degrade FEL performance when the beam size becomes too small. Therefore, the beam size—and thus the β-function—needs to be chosen properly to optimize the FEL performance. Using Ming-Xie's FEL fitting formula [6] we find that the shortest gain length for our case is obtained when average $\beta = 6$ m; for our simulations, however, we back off and choose $\beta = 10$ m. To accommodate this choice we place quads between undulator sections, where each section is taken to be 2 m long, with breaks of 30 cm between sections.

SIMULATIONS

For both cases of charge ($Q = 250, 20$ pC) the beam was first tracked, using the computer program ELEGANT [7], from the beginning of the linac to the beginning of the undulator, as was described in [3]. The peak current at the A-Line undulator can be adjusted by setting the rf phase of Linac-2 of the LCLS (upstream of BC2, the 2nd bunch compressor [1]). An important feature of the linac is that this phase can be set independently for the A-Line beam and the main (hard X-ray) LCLS beam. In this way the peak current is set independently for the two beams. In fact, unlike the main beam, the A-Line beam is over-compressed

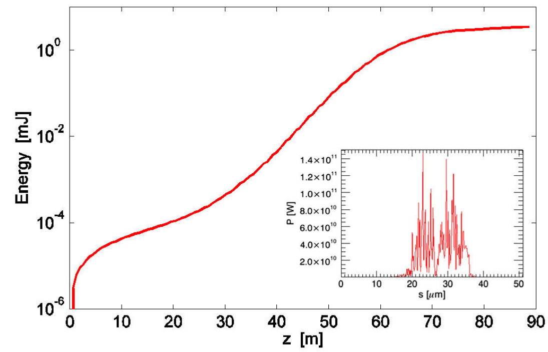

Figure 1: Radiation energy along the undulator for the 250 pC beam. The temporal profile of the pulse at saturation is given in the inset. The radiation saturates at $z = 70$ m with an energy of $E_{FEL} = 2$ mJ. The peak power reaches to more than 100 GW at saturation.

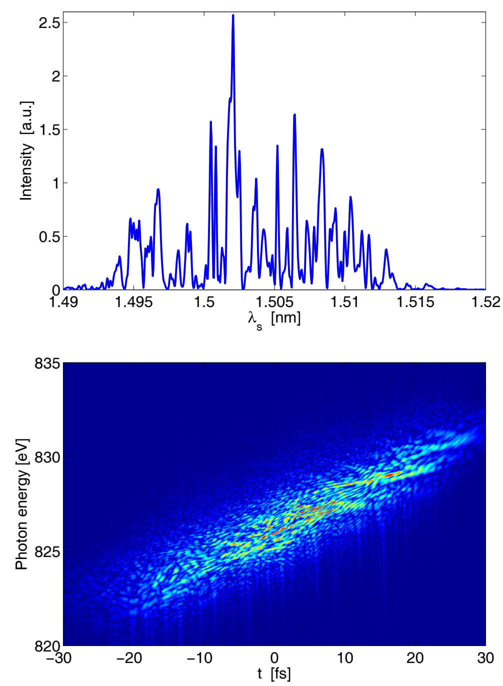

Figure 2: The radiation spectrum (top) and longitudinal phase space (bottom) at saturation for the 250 pC beam. A frequency chirp, derived from the energy chirp of the electron beam, can be seen clearly in the bottom plot.

in BC-2, in order to mitigate CSR effects (see Ref. [3]). Note also that because the arc in the A-Line is used for final compression, the electron bunch arrives at the undulator with a roughly linear residual energy chirp. The magnitude of the chirp is dictated by the charge and bunch length desired at the entrance to the undulator. For the 250 pC case, at the beginning of the A-Line undulator, the bunch longitudinal distribution is approximately Gaussian with peak current I_{pk} =3.5 kA, rms bunch length $\sigma_{zf} = 10$ μm, and slice emittances $\epsilon_{xs} = 1.0$ μm, $\epsilon_{ys} = 0.7$ μm; the slice energy spread $\sigma_{\delta s} = 10^{-4}$ while the beam energy spread $\sigma_\delta = 5 \times 10^{-3}$ [3]. The beam quality has been well preserved during transport.

After tracking to the beginning of the A-Line undulator, the beam properties are passed from ELEGANT to GENESIS [8], a 3D time-dependent FEL code, in order to evaluate the FEL performance. Figure 1 shows the FEL radiation energy along the undulator length at $\lambda_s = 1.5$ nm. The FEL energy saturates at $z = 70$ m with a saturation energy of $E_{FEL} = 2$ mJ. The temporal profile of the radiation pulse at saturation is also shown in Fig. 1 (the inset). The peak power $P_{FEL} \sim 100$ GW and the radiation pulse length (FWHM) $\Delta\tau = 50$ fs. The residual energy chirp in the beam is not expected to inhibit lasing; however, it will induce a corresponding frequency chirp $\Delta\lambda_s/\lambda_s \sim 2\Delta\gamma/\gamma \sim 1\%$ here. This phenomenon can be seen from the radiation spectrum (top plot) and longitudinal phase space (bottom plot) shown in Fig. 2. It is possible that the chirp can be accommodated and perhaps even used to advantage in the design of experiments.

For the 20 pC configuration the bunch longitudinal distribution at the entrance of the undulator is again approximately Gaussian but with a peak current I_{pk} =4.0 kA, rms bunch length $\sigma_{zf} = 1$ μm, and slice emittances $\epsilon_{xs} = 0.7$ μm, $\epsilon_{ys} = 0.2$ μm; the slice energy spread $\sigma_{\delta s} = 10^{-4}$ and the beam energy spread $\sigma_\delta = 5 \times 10^{-3}$ (the beam again has a residual energy chirp) [3]. For this configuration Fig. 3 shows the FEL radiation energy as function of z at wavelength $\lambda_s = 1.5$ nm. The FEL energy saturates at $z = 50$ m with a saturation energy of $E_{FEL} = 0.1$ mJ, much less than the 2 mJ we found for the 250 pC case, due to much smaller bunch charge. The temporal profile of the radiation pulse at saturation is also shown in Fig. 3 (in the inset). The peak power $P_{FEL} \sim 70$ GW and the radiation pulse length (FWHM) $\Delta\tau = 2$ fs.

The radiation spectrum and longitudinal phase space are shown in Fig. 4 (respectively in the top and bottom plots). Note that, unlike in the 250 pC case, there is no frequency chirp in the longitudinal phase space of the radiation. This is because the beam energy spread ($\sim 10^{-4}$) is now much less than the FEL bandwidth ($\sim 0.2\%$ FWHM), and therefore the frequency chirp becomes smeared by the FEL process.

For the 20 pC case we also studied the pulse-to-pulse fluctuation in radiation at a wavelength of 1.5 nm using a 1D FEL simulation code that we have written. The beam parameters were slightly modified from the ones used in Genesis, so that the radiation has comparable gain lengths in 1D and 3D. The result was obtained by doing statistics over 1000 independent runs. The rms variation in power *vs.* z/L_g, with L_g the 1D gain length, is shown in Fig. 5, the blue curve. The radiation at 1.5 nm is not quite a single spike. A single longitudinal mode, however, can be obtained at longer wavelength, such as at 3 nm. Fig. 5 also gives the rms variation in power for this wavelength (the red curve). We can see that in the exponential gain region the fluctuation at 3 nm is much higher than at 1.5 nm; after saturation, however, they both quickly drop to the same level, $\sim 15\%$.

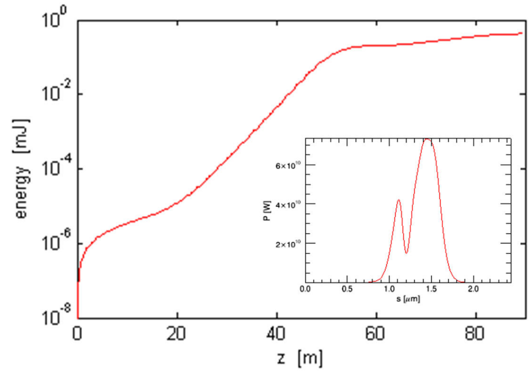

Figure 3: Radiation energy along the undulator for the 20 pC beam. The temporal profile of the pulse at saturation is given in the inset. The radiation saturates at z ~50 m with a saturation energy of E_{FEL} ~0.1 mJ. The peak power reaches more than 70 GW at saturation.

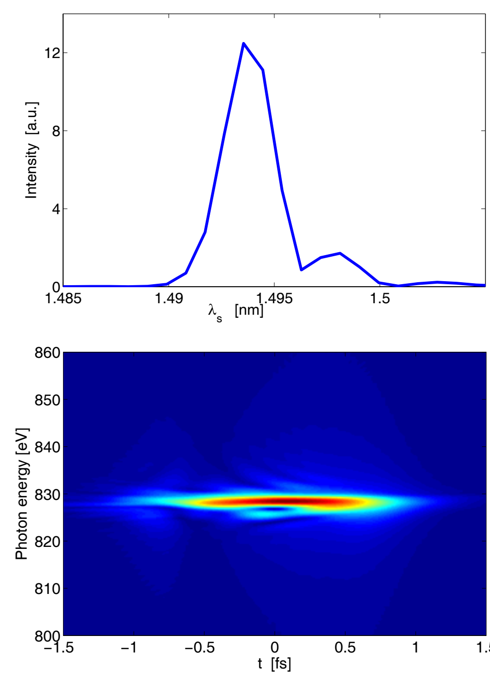

Figure 4: The radiation spectrum (top) and longitudinal phase space (bottom) at saturation for the 20 pC beam. Notice that, in this case, there is essentially no chirp in the radiation.

Finally we performed simulations for a 250 pC beam and for the shortest wavelength under consideration for the A-Line, $\lambda_s = 1$ nm. In this case we find that the radiation reaches saturation at $L_g \sim 80$ m. A shorter saturation length could be achieved by compressing the beam more, to a higher current. With the more advanced technology of a superconducting undulator, the radiation wavelength may even be able to be pushed further down, to 0.5 nm, with a

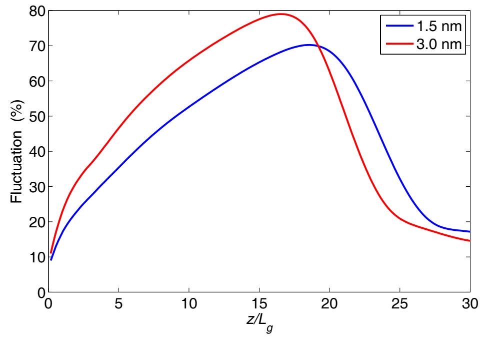

Figure 5: Fluctuation in the power along the undulator for radiation wavelengths $\lambda_r = 1.5, 3.0$ nm, when $Q = 20$ pC. The plot gives the rms variation in power obtained from 1000 independent runs. The abscissa is normalized to the 1D gain length L_g.

saturation length of just $\sim$ 40 m (as will be shown in the following section).

SUPERCONDUCTING HELICAL UNDULATOR

A helical undulator produces circularly polarized X-rays. The high peak field of a helical device would produce more spontaneous radiation than has been experienced with LCLS undulator; however, the radiation spectrum for a helical undulator will have no harmonics of the fundamental wavelength.

For the purposes of this study, we have based our calculations on a 4 cm period, superconducting helical undulator that can reach 3.55 T on axis. Figure 6 shows the estimated (using Ming Xie's fitting formula [6]) saturation length for a radiation spectrum of $\lambda_s = 0.5$–5 nm, assuming energy $E_0 = 13.6$ GeV, peak current $I_{pk} = 3.5$ kA, slice emittance $\epsilon_{xs} = 1.0\ \mu$m, slice energy spread $\sigma_{\delta s} = 10^{-4}$, and beta function $\langle\beta\rangle = 10$ m. We can see that the wavelength range 0.5–5 nm can be spanned with an undulator that occupies only $\sim$ 40 m.

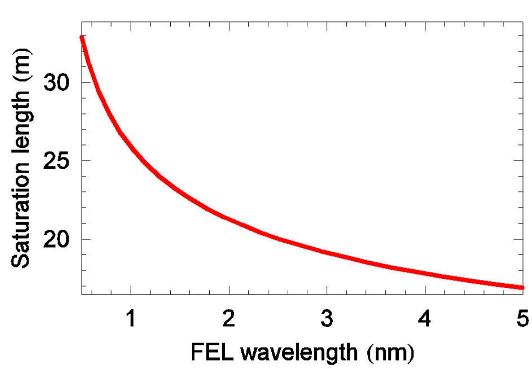

Figure 6: Saturation length *vs.* wavelength as obtained by Ming Xie's fitting formula for the $Q = 250$ pC case.

We are aware that superconducting undulator technology is presently not ready for FEL use, due to the tight tolerances on phase error, trajectory straightness, and other factors [9]. But if an investment is made in developing a superconducting helical undulator that satisfies all the tolerances, the short-wavelength limit of the A-Line soft X-ray FEL may be able to be extended to 0.5 nm with an undulator that is only 40 meters long. Then one could consider using the extra 40 m of free space for a second harmonic afterburner [10], polarization control [11], or FEL seeding.

CONCLUSION

We have investigated the use of the SLAC A-Line as a new, soft X-ray FEL (1–5 nm) that would share beam pulses with and complement the spectral range of the existing LCLS hard X-ray FEL. In an earlier report, beam transport from the SLAC linac up to the position of a new undulator in the A-Line was studied; in the present report, the actual performance of the new FEL was investigated. The undulator we consider is a conventional planar, permanent magnet type, with a period of 8 cm and a total length of 80 m. We have performed simulations for a radiation wavelength of 1.5 nm. We have shown that for the nominal LCLS bunch charge (250 pC), lasing can be achieved with peak power 100 GW, pulse length 50 fs, and radiation energy 2 mJ, and the radiation possesses a 1% frequency chirp. In a low charge configuration (20 pC), we have peak power of 70 GW, pulse length of 2 fs, and energy of 0.1 mJ, and in this case there is no frequency chirp.

Finally we studied the possibilities of using a superconducting helical undulator to increase the wavelength reach of the A-Line FEL. Assuming an improvement in tolerances available with superconducting undulators, we envision in the near future in the A-Line a spectrum reach of 0.5–5 nm and a saturation length of only 40 m by using such technology.

ACKNOWLEDGEMENTS

We thank K. Bane for careful reading and editing the text. H. Geng also would like to thank D. Ratner for helping with the spectrum analysis. This work was supported by Department of Energy Contracts No. DE-AC02-76SF00515 and the China Scholarship Council.

REFERENCES

[1] P. Emma, Commissioning Status of the LCLS X-Ray FEL, PAC '09 proceedings, 2009.
[2] The Stanford Two-Mile Accelerator, R.B. Neal, Editor (1968).
[3] H. Geng et al., Optics Design for a Soft X-ray FEL at the SLAC A-Line, PAC '09 proceedings, 2009.
[4] Y. Ding et al., PRL 102, 254801 (2009).
[5] R. Bonifacio et al., Opt. Commun. 50, 373 (1984).
[6] M. Xie, LBL Preprint No-36038, 1995.
[7] M. Borland, ELEGANT, Advanced Photon Source LS-287, 2000.
[8] S. Reiche et al., Nucl. Instrum. Methods Phys. Res. Sect. A 429, 243 (1999).
[9] S. Prestemon, private communication.
[10] Z. Huang, S. Reiche, FEL '04 proceedings, 2004.
[11] Y. Ding, Z. Huang, Phys. Rev. ST-AB 11, 030702 (2008).